



HAL
open science

Mobility of organic compounds in a soft clay-rich rock (Tégulines clay, France)

Ning Guo, Zoé Disdier, Emilie Thory, Jean-Charles Robinet, Romain Dagnelie

► **To cite this version:**

Ning Guo, Zoé Disdier, Emilie Thory, Jean-Charles Robinet, Romain Dagnelie. Mobility of organic compounds in a soft clay-rich rock (Tégulines clay, France). *Chemosphere*, 2021, 275, pp.130048. 10.1016/j.chemosphere.2021.130048 . cea-03540711v2

HAL Id: cea-03540711

<https://cea.hal.science/cea-03540711v2>

Submitted on 10 Oct 2023

HAL is a multi-disciplinary open access archive for the deposit and dissemination of scientific research documents, whether they are published or not. The documents may come from teaching and research institutions in France or abroad, or from public or private research centers.

L'archive ouverte pluridisciplinaire **HAL**, est destinée au dépôt et à la diffusion de documents scientifiques de niveau recherche, publiés ou non, émanant des établissements d'enseignement et de recherche français ou étrangers, des laboratoires publics ou privés.



Distributed under a Creative Commons Attribution - NonCommercial 4.0 International License

**Mobility of organic compounds in a soft clay-rich rock
(Tégulines clay, France)**

Ning Guo ^a, Zoé Disdier ^a, Émilie Thory ^a,

Jean-Charles Robinet ^b, Romain V.H. Dagnelie ^{a,*}

(a) Université Paris-Saclay, CEA, Service d'Étude du Comportement des Radionucléides, 91191, Gif-sur-Yvette, France

(b) Andra, R&D Division, parc de la Croix Blanche, 92298, Clamart-Malakoff, France

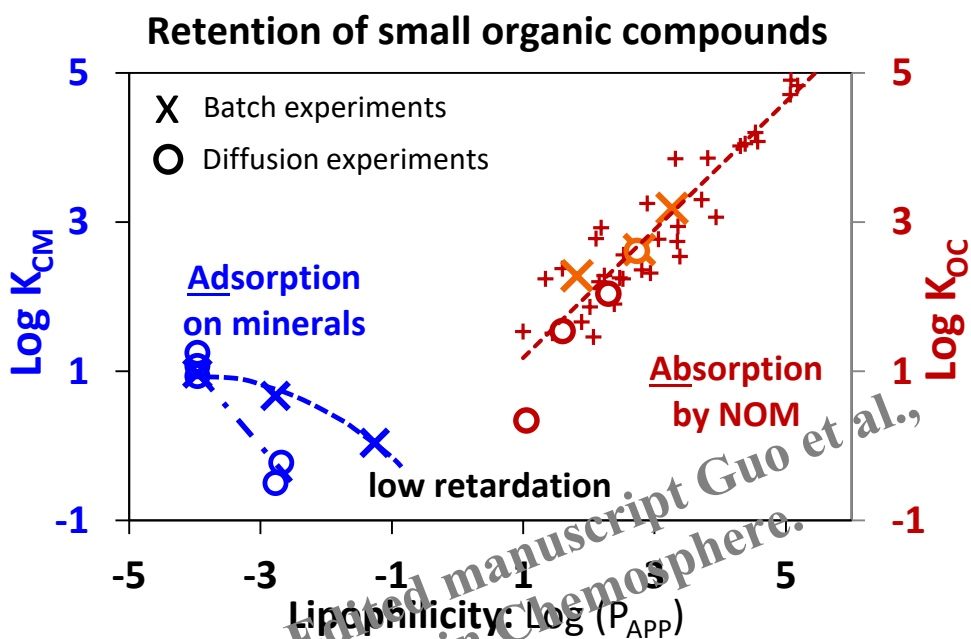
*Preprint version. Edited manuscript Guo et al.,
2021, published in Chemosphere.*

* Corresponding author. Université Paris-Saclay, CEA/DES/ISAS/DPC/SECR/L3MR, 91191, Gif-sur-Yvette, France. *E-mail address:* **romain.dagnelie@cea.fr**

Highlights:

- Transport of organic compounds is quantified in a soft clay rock (Tégulines)
- Low content of organic matter drives the retention of lipophilic compounds
- Retention of ionizable sorbates decreases with lipophilicity ($\log P_{OW} < 0$)
- Apparent partition coefficient, P_{APP} , are reported for ionizable compounds
- Diffusion coefficients provide contribution of charge and size to porosity exclusion

Graphical Abstract



Abstract

The migration of organic compounds in soils is a major concern in several environmental issues. Contaminants display distinct behaviours as regards to their specific affinities towards soils constituents. The retention mechanism of hydrophobic compounds by natural organic matter is well known. The retention of ionizable compounds is mainly related to oxides and clay minerals, even if less documented in reductive media. In this work, we investigated the migration of organic compounds in a soft clay-rich sedimentary rock (Tégulines clay, France). The aim was to determine the relative contributions of natural sorbents on retention, and eventual correlations with solutes properties. Both hydrophobic compounds (toluene, benzene, naphthalene) and hydrophilic species (adipate, oxalate, ortho-phthalate, benzoate) were investigated, using batch and diffusion experiments.

The retention of neutral aromatic compounds correlates with their lipophilicity ($\log P_{OW}$), confirming that absorption mechanism prevails, despite a low content of natural organic matter ($\leq 0.5\%$). A low retention of ionizable compounds was quantified on Tégulines clay. The eventual discrepancies between data acquired on crushed rock and solid samples are discussed. Low effective diffusion coefficients are quantified. These values hint on the relative contributions of steric and electrostatic exclusion, despite a large pore size in such “soft” clay-rock. Overall, the dataset illustrates a general scheme for assessing the migration over a wide variety of organic compounds. This approach may be useful for predictive modelling of the fate of organic compounds in environmental media.

Keywords:

Clay rock, Organic compound, Adsorption, Absorption, Diffusion, Anion exclusion

Abbreviations and notations:

α : Apparent porosity (diffusion accessible)

ϵ : Porosity of media

Π : Exclusion factor from porous media

COx: Callovian-Oxfordian (Clay rock)

D_0 : Diffusion coefficient ($\text{m}^2 \text{s}^{-1}$) in water

D_e : Effective diffusion coefficient ($\text{m}^2 \text{s}^{-1}$) in porous media

$f_{\text{OM}} / f_{\text{CM}}$: Massic fraction of organic matter / clay minerals in sorbents

HDO: Semi-heavy water

IS: Ionic strength

K_{CM} : Contribution of clay minerals to the solid-liquid distribution coefficient ($\text{L kg}(\text{clay})^{-1}$)

K_{OC} : Contribution of organic matter to the solid-liquid distribution coefficient ($\text{L kg}(\text{NOM})^{-1}$)

NOM: natural organic matter

OPA: Opalinus (clay rock)

Orga: Organic (compound / sorbate)

P_{APP} : Apparent octanol water partition coefficient

P_{OW} : Octanol water partition coefficient (analogue to K_{OW})

R_d : Solid-liquid distribution coefficient (L kg^{-1})

1. Introduction

The transport of organic compounds in environmental media is studied for various applications: extraction of fossil fuels, fate of emerging organic contaminants, waste disposal and remediation of soils. The term “organic” may be misleading, as it corresponds to a large diversity of compounds: small ionizable compounds such as amino-acids, hydrophobic or hydrophilic hydrocarbons, large synthetic or natural geopolymers and natural organic matter (NOM) such as fulvic and humic acids. This work focuses on the transport of small soluble molecules in the near surface of geological systems. Both ionizable carboxylic acids and neutral aromatic compounds are investigated. The migration of such solutes in sedimentary rocks is highly sensitive to sorption leading to diffusive retardation (Altmann et al., 2012; Shackelford and Moore, 2013). Sorption-influenced transport is largely described in literature for organic compounds (Borisover and Davis, 2015; Schaffer and Licha, 2015) indicating that the retention part may originate from various mechanisms. Hydrophobic compounds, such as alkanes and aromatic compounds are mainly absorbed by NOM (Borisover and Graber, 1997; Karickhoff, 1981) with Freundlich-type sorption isotherm, eventually leading to intra-particulate slow diffusion mechanism (Pignatello and Xing, 1996). On contrary, hydrophilic compounds such as ionizable molecules are adsorbed on the surfaces of minerals, e.g. clays and oxides (Gu et al., 1994; Hwang et al., 2007; Johnson et al., 2004; Kang and Xing, 2007). Adsorption may be assumed in this case, with instantaneous and reversible Langmuir-type isotherms, leading to increased apparent porosity and diffusive retardation factor. Both mechanisms of adsorption and absorption, may occur simultaneously on the various mineralogical components of a natural medium, but the relative contribution of these mechanisms is rarely discussed.

Clay rock geological formations are considered in several countries for hosting a radioactive waste disposal, e.g. Callovian-Oxfordian (COx) and Tégulines in France, Opalinus Clay (OPA) and Helvetic Marl in Switzerland, Boom Clay in Belgium, etc. (Altmann et al., 2012; Appelo et al., 2010;

Maes et al., 2011). The COx clay rock has been extensively studied in the context of the French Geological Radioactive Waste Disposal (Cigéo project). Corresponding studies investigated the interaction between inorganic or organic solutes and COx clay rock (Descostes et al., 2008; Melkior et al., 2007; Rasamimanana, 2017a; Savoye et al., 2012). Absorption of neutral hydrophobic compounds occurs in NOM (Vinsot et al., 2017), with an eventual contribution from clay minerals (Willemsen et al., 2019). Similarly, the adsorption of organic anions occurs on clayey minerals, despite a positive charge on clayey mineral surfaces (Rasamimanana et al., 2017b). Still, electrostatic interactions between mineral surfaces and solutes leads to a partial exclusion of anions from rock porosity. This so-called “anion exclusion” decreases both effective diffusion coefficient and retardation factor of anions, as compared to neutral solutes (Chen et al., 2018; Dagnelie et al., 2018). However, some major discrepancies are observed between data measured by sorption on crushed clay rock and retardation factor observed in solid samples. For that reason, the quantification of diffusive retardation factors seems mandatory.

This work focuses on the Tégulines clay, from the Albian Gault geological formation (East Paris Basin, France) under investigation for a potential near surface geological radioactive waste repository (Lerouge et al., 2018; Missana et al., 2017). This repository would confine low-activity long-lived waste, such as ^{14}C -graphite, remain from old natural uranium graphite gas nuclear power reactor, developed in France until the 90s. In absence of exhaustive characterization, the organic source term potentially released by radiolytic lixiviation of graphite waste makes both neutral and anionic reference compounds being of interest (Andra, 2015; Pageot et al., 2016, 2018; Poncet and Petit, 2013). The purpose of this work is to quantify sorption and retardation factors of various organic species, in order to assess the confinement properties of the geological barrier toward potential release of ^{14}C bearing compounds. To that aim, diffusion experiments were performed and compared to sorption experiments or predictive model based on media mineralogy. Moreover, the comparison between results on Tégulines “soft” clay rock and COx “hard” clay rock, displaying different compactions, are interesting to assess potential porosity exclusion and effects on sorption-influenced transport of anions.

2. Material and methods

2.1. Rock samples

Experiments were carried out on Tégulines clay samples from the Albian Gault clay formation. Rock samples were collected from two boreholes (AUB01918, AUB01825). The cores were drilled at depths -20 and -22 m from the surface of the studied area (NE-SW) in the eastern part of the Paris Basin (France) (Amédéo et al., 2017; Lerouge et al., 2018 and 2020). The mineralogical composition is detailed in supplementary data (Table S1). It is basically composed of 50% of clay minerals, 40% of quartz, less than 5% of calcite and 0.6% of NOM. After drilling, the core samples were protected from oxygen using container with $\text{N}_{2(\text{g})}$. They were manipulated inside a glovebox ($P_{\text{O}_2}/P_0 < 2$ ppm) to prevent mineral oxidation. The hydrated and “pasty” outlayer of the core was firstly removed and the inner sound part of the rock was kept. The inner core was then sliced using a wire saw into disk samples with a thickness of ~ 10 mm, and a diameter of ~ 35 -40 mm. The metrology of the samples used in diffusion cells is provided in supplementary data (Table S2). These measurements indicate an average hydrated density $\sim 1.98 \pm 0.10$ g cm^{-3} . The difference between this hydrated density and clay rock dry density $\rho^{\text{dry}} \sim 1.7$ g cm^{-3} provides a rough estimation of rock porosity: $\varepsilon = 28 \pm 10\%$. This value is in agreement with the results obtained from diffusion experiments detailed subsequently. Some of the remaining off-cut were crushed and sieved entirely below 125 μm for batch experiments.

A synthetic pore water was prepared by dissolution of pure salts (purity $> 99.5\%$) to reach the composition for underground pore water of Gault formation clay rock (Ionic strength: $\text{IS} = 2.33 \cdot 10^{-2}$

M, equilibrated $\text{pH} = 7.2 \pm 0.2$, Table S3). The synthetic water was bubbled (1 L min^{-1}) with a mix of N_2/CO_2 (99/1) for more than 2 hours, removing O_2 and equilibrating dissolved CO_2 . The synthetic pore water was then mixed with “sacrificial” crushed clay rock with a solid to liquid ratio of 10 g L^{-1} and agitated for more than 48 h. This step was used for the equilibration of trace elements such as Fe, Al, Mn, Si and NOM. Equilibrated pore water was filtrated through a $0.8 \mu\text{m}$ membrane to remove the sacrificial clay. Additional filtration step through a $0.22 \mu\text{m}$ membrane was processed before experiments to prevent bacterial activity. The composition of the equilibrated synthetic water was analysed by ionic chromatography (Metrohm, 850 IC). Alkalinity was measured by acidic dosage (HCOOH) in presence of methylene blue (Sarazin et al., 1999) with a UV-vis spectrophotometer (Cary-500 from Agilent). The prepared pore water was used for pre-equilibration step of clay samples, as described in the following section.

2.2. Adsorption experiments

The crushed clay ($< 125 \mu\text{m}$) was equilibrated for more than 48 hours with synthetic pore water in sealed polycarbonate centrifugation tubes, with a solid to liquid ratio of 250 g L^{-1} (1.5 g in 6 mL). Each tube was then spiked with ^{14}C or ^3H -organic tracer and agitated in a shaking machine for 24 h at least, and up to 7 days. At the time of sampling, the tubes were centrifuged over $50,000 \text{ g}$ for 1 h and a fraction of the supernatant was sampled. The tracer activity was determined by liquid scintillation counting on 1 mL samples (Packard TRICARB 2500), after addition of 4 mL of liquid scintillation solution (ultima goldTM cocktail). The mass balance was checked for each tracer by duplicate experiments, i.e. without clay. The variation of blank activity was below measurement accuracy ($\Delta A_0 < 2 \%$). All organic molecules studied in this work and their properties are displayed in Table 1. Aromatic and small carboxylic acids were chosen as compounds potentially released by degradation of graphite. The compounds were also chosen in order to cover a wide range of lipophilicity ($-4 < \log D < 3.5$). The equilibrium concentration range was limited by the solubility of the organic compound in aqueous solution and the specific activity of radioactive sources. When available, full sorption isotherms cover a wide range of concentrations, thus providing information on sorption process, e.g. isotherm shape and saturation of sorption sites (Langmuir, Freundlich, etc.).

Table 1 Properties of organic molecules. P_{OW} is the octanol water partition coefficient of carboxylic acids (RCOOH). $\log P_{APP}$ is the apparent partition coefficient in Tégulines pore water (pH \sim 7.2). $*pH^{EXP.} = 7.7 \pm 0.2$. Recommended values are in bold. $^{\$}$ Structure of molecules detailed in Table S4. [1] (Haynes, 2014), [2] (Hansch et al., 1995), [3] (Pinsuwan et al., 1995), [4] (Sangster, 1989).

Compound	Name (IUPAC)	Formula $^{\$}$	Mw (g mol $^{-1}$)	$pK_a^{[1]}$	Charge (pH 7.2)	$\log P_{OW}^{[2,3,4]}$	$\log P_{APP}$ (Théor.)	$\log P_{APP}$ (Exp.)
o-phthalate	Benzene-1,2-dicarboxylic acid	C ₈ H ₆ O ₄	166.14	2.94, 5.43	Ph. ²⁻	0.73	-5.3	-2.77 \pm 0.2*
Oxalate	Oxalic acid	C ₂ H ₂ O ₄	90.03	1.25, 4.14	Ox. ²⁻	-0.47	-9.5	-3.96 \pm 0.2*
Benzoate	Benzoic acid	C ₇ H ₆ O ₂	122.12	4.20	Bz ⁻	1.87	-1.13	-1.26 \pm 0.2*
Adipate	Hexanedioic acid	C ₆ H ₁₀ O ₄	146.14	4.43, 5.42	Ad. ²⁻	0.08	-4.5	n.d.
Naphthalene	Naphthalene	C ₁₀ H ₈	128.17	aprotic	N ⁰	3.32	3.4	3.3 \pm 0.1
Toluene	Toluene	C ₇ H ₈	92.14	aprotic	T ⁰	2.73	2.7	2.77 \pm 0.1
Benzene	Benzene	C ₆ H ₆	78.11	aprotic	B ⁰	2.13	2.1	1.82 \pm 0.1

2.3 Diffusion experiments

Six diffusion experiments were conducted in typical through-diffusion cells (numbering provided in Table 2), with a geometry detailed in Descostes et al., (2008) and provided in Fig. S3. Prior to diffusion experiments, the rock samples were pre-equilibrated by filling both upstream and downstream reservoirs with synthetic pore water. Clay was then equilibrated more than 48h and solutions renewed several times in order to ensure chemical equilibrium. Semi-heavy water (HDO) was used as a conservative reference, i.e. non sorbing tracer with access to the whole porosity. To that aim, upstream solutions were spiked with heavy water (D₂O). Both compartments were then periodically sampled. HDO content was measured by infrared laser spectrometry (LGR, DLT-100 from Los Gatos Research). After sampling, the upstream volume was renewed with initial injection solution and downstream volumes renewed with raw pore water. After a few weeks of monitoring, upstream solution was renewed by a solution with labelled organic tracers. The initial concentrations of organics were controlled by Total Organic Carbon analysis (Vario TOC Cube from Elementar) for cold solutions. Through-diffusion of organic compounds was monitored following the same procedure than for HDO, except that samples were measured by liquid Scintillation Counter (Packard TRICARB 2500 with ultima goldTM, Perkin Elmer).

2.4 Data modelling

Distribution between liquid and solid may follow two mechanisms: absorption or adsorption. Absorption is a process in which an absorbate (atoms, molecules or ions) goes into a bulk phase of absorbent. The mechanism at the interface can be considered as a partitioning in two immiscible phases. Adsorption is a surface phenomenon, with an “increase in the concentration of a substance at the interface between a condensed material (sorbent) and in our case a liquid phase. Both absorption and adsorption can be quantified by a solid-liquid distribution coefficient, R_d (L kg⁻¹):

$$R_d = \frac{q_e}{c_e} \quad (1)$$

where q_e (mol kg⁻¹) is the concentration of sorbed species per mass of sorbent, and C_e (mol L⁻¹) the concentration in solution at equilibrium with the solid. In this work, the solid-liquid distribution coefficient R_d (L kg⁻¹) is calculated using the following Eq. (2):

$$R_d = \left(\frac{C_0}{C_{eq}} - 1 \right) \times \frac{V}{m} = \left(\frac{A_0}{A_{eq}} - 1 \right) \times \frac{V}{m} \quad (2)$$

with C_0/C_{eq} (mol L⁻¹) being the initial/equilibrium concentrations in solution; A (Bq) the activity, assumed proportional to C at any time; V (mL) the solution volume; and m (g) the dry mass of clay rock. The uncertainty (u) on R_d values is calculated using uncertainties on previous parameters through the Eq. (3):

$$u_{R_d}^2 = \left(\frac{V}{m \times A_{eq}} \right)^2 u_{A_0}^2 + \left(-\frac{A_0 V}{A_{eq}^2 m} \right)^2 u_{A_{eq}}^2 + \left(\frac{R_d}{V} \right)^2 u_V^2 + \left(\frac{R_d}{m} \right)^2 u_m^2 \quad (3)$$

Sorption isotherms can be described by several empirical equations. For example, Langmuir and Freundlich isotherms are described by Eq. (4) and Eq. (5), respectively, with K_L ($L \text{ mol}^{-1}$), K_F ($L^{(1/n)} \text{ kg}^{-1} \text{ mol}^{(1-1/n)}$), the affinity constants, and Q (mol kg^{-1}) the maximum sorbed amount. Langmuir-type isotherm is usually observed when adsorption occurs with a single energy interaction, leading to surface monolayers. Such behavior was evidenced by adsorption of hydrophilic organic molecules on COx clay rock (Rasamimanana et al., 2017a). Freundlich isotherm is more common when several interactions occur, e.g. including multilayer or absorption processes. The parameter $1/n$ can be seen as a sorption intensity (Karnitz et al., 2007). When $n = 1$, the Freundlich isotherm, Eq. (5), becomes analogue to partitioning, $R_d = K_F = C_{\text{org}}/C_{\text{eq}}$. In this work, Eq. (4) and Eq. (5) are respectively applied to describe the adsorption of hydrophilic organic molecules and absorption of lipophilic organic molecules in Tégulines clay rock.

$$q_e = Q \times \frac{K_L \times C_e}{1 + K_L \times C_e} \quad (4)$$

$$q_e = K_F \times C_e^{1/n} \quad (5)$$

The one dimensional analysis of diffusion results is based on Fick's second law (Crank, 1975), described by Eq. (6):

$$\frac{\partial C}{\partial t} = \frac{D_e}{\varepsilon_a + \rho(1-\varepsilon)R_d} \frac{\partial^2 C}{\partial x^2} = \frac{D_e}{\alpha} \frac{\partial^2 C}{\partial x^2} \quad (6)$$

with C represents the tracer concentration (mol L^{-1}), t the time (s), D_e the effective diffusion coefficient ($\text{m}^2 \text{ s}^{-1}$), ε and ε_a are the total and diffusion accessible porosities, ρ is the grain density of Tégulines clay rock ($\sim 1.7 \text{ kg L}^{-1}$), $\alpha = R \times \varepsilon$ is called the rock capacity factor. The normalized flux of tracer, J^{NORM} ($\text{m}^2 \text{ s}^{-1}$) is defined by Eq. (7):

$$J_{\text{down}}^{\text{NORM}}(t) = \frac{L}{C_0} \frac{dn_{\text{down}}(t)}{S \times dt} \quad (7)$$

where dn_{down} is the quantity of tracer reaching the downstream reservoir (moles), per unit of time dt (s), and per sample surface S (m^2), L (m) the thickness of sample, and C_0 (moles m^{-3}) the initial upstream concentration.

The effective diffusion coefficient (D_e) and the rock capacity factor (α) are adjusted by least-square fitting of both downstream flux and depletion of the upstream concentration. The mass balance was assessed by comparison between upstream experimental data and modelling. Satisfactory mass balances, $\Delta C \ll 5\%$, were obtained for all experiments, except for toluene (Cell n° 6) which is discussed furtherly. Data and modelling for the reference tracer, HDO, are provided in Fig. S4. The average values of D_e and ε for HDO obtained from the 6 samples are $D_e = (1.38 \pm 0.37) \times 10^{-10} \text{ m}^2 \text{ s}^{-1}$ and $\varepsilon = 0.41 \pm 0.06$.

3. Results

3.1. Sorption of organic compounds on Tégulines clay

The Fig. 1 shows the experimental sorption results on Tégulines clay rock. R_d values of ionizable compounds are rather constant as a function of equilibrium concentration. The corresponding average value, R_d^{EXP} , for each organic compound are gathered in Table 3. Some compounds display

significant affinities (i.e. $\rho \times R_d \gg \varepsilon$). For example, the value R_d (oxalate) = 4.7 L kg⁻¹ is one order of magnitude higher than that of benzoate.

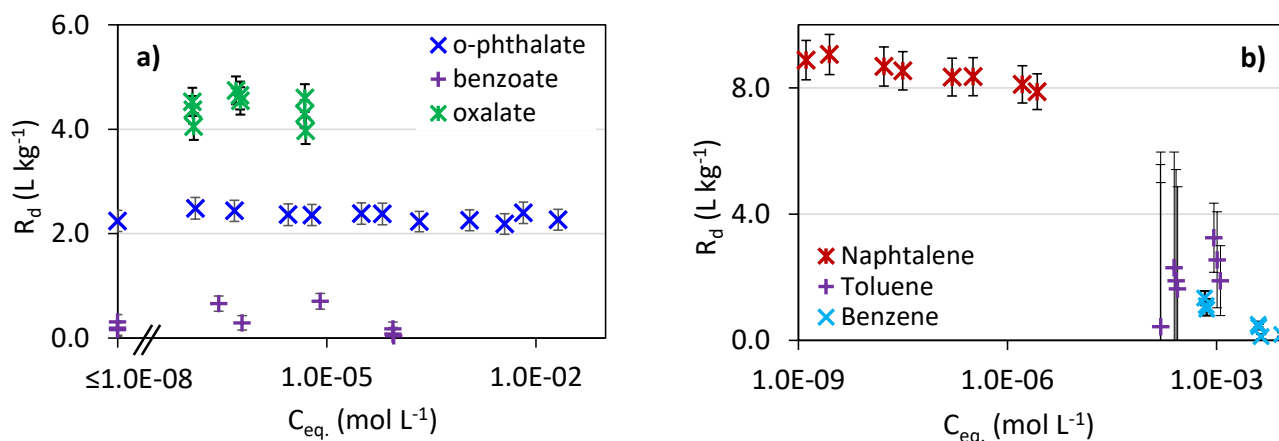


Fig. 1. Solid-liquid distribution coefficients (R_d) of organic compounds on Tégulines clay rock as a function of equilibrium concentration. $V/m = 4$ L kg⁻¹, $\text{pH} = 7.2 \pm 0.2$, $T = 22 \pm 2^\circ\text{C}$.

(a) Data for ionizable compounds: o-phthalate, benzoate and oxalate.

(b) Data for neutral aromatic compounds: naphthalene, toluene and benzene.

The sorption isotherm of phthalate also displays a rather constant value. No clear saturation of sorption site is observed in the range of concentration measured, as expected in Langmuir-type shape (Eq. (4), Rasamimanana et al., 2017a). The best-fit modelling is provided in supplementary information (Fig. S2). Adjusted values are $Q = 1.5 \pm 2.1$ mol kg⁻¹, and $K_L = 1.6 \pm 2.2$ L mol⁻¹, leading to $R_d^{\text{MAX}} \sim K_L \times Q = 2.3 \pm 4.5$ L kg⁻¹. The o-phthalate compound displays higher affinity to Tégulines clay rock than benzoate. This highlights the role of the di-carboxylate group on sorption mechanism (Rasamimanana et al., 2017a). Still, phthalate displays a weaker adsorption than oxalate, eventually linked to a steric effect, as discussed in Section 4.

The Fig. 1 also illustrate the sorption of neutral organic compounds on Tégulines clay rock. The R_d^{EXP} values of neutral organic compounds are displayed in Table 3, and exhibit with an order of naphthalene > toluene > benzene. The value R_d (naphthalene) = 9.1 L kg⁻¹, is one order of magnitude higher than that of benzene. These R_d values, from 1.14 to 9.10 L kg⁻¹ are similar to that for ionizable compounds, despite rather different retention mechanism. Indeed, a slight decrease of R_d values is observed with the equilibrium concentration. Typical Freundlich isotherm, Eq. (5), was used to explain the naphthalene sorption isotherm, as illustrated in Fig. S2. The best fitting parameters are $K_F = 6.9 \pm 0.2$ and $n = 1.0$. The value of the constant $n = 1$ indicates a constant energy interaction and a sorption mechanism such as absorption (i.e. partitioning between two phases). The constant value of R_d in this range of concentration allows the use of similar equations for both ionizable and neutral compounds for modelling of diffusion experiments.

3.2. Diffusion of organic compounds in Tégulines clay rock

The results of through-diffusion experiments are illustrate in Fig. 2. A depletion of upstream concentration and accumulation in downstream compartment (i.e. positive flux) is observed with time increasing. Phthalate was observed in the downstream during the first day, much earlier than adipate (~3

days) and oxalate (~15 days). This indicates a low retardation factor and retention for o-phthalate. On contrary, toluene was detected in the downstream after 14 days, indicating a higher retention. In the case of toluene, the non-linear sorption isotherm leads to a slight deviation between observed and model data and an “apparent” bias in mass balance. This does not affect significantly further estimation of the retardation factor, based on the normalized flux. For other compounds, the model agreement between both upstream and downstream data validates the model hypothesis, as well as mass balance of the experiment.

For all compounds, a “steady state” is reached after a few tens of days, meaning a constant flux of tracer. The normalized fluxes, calculated from downstream data with Eq. (7), are shown in Fig. 2. The value of the plateau provides a visual estimation of effective diffusion coefficients (D_e). The D_e of organic compounds in Tégulines clay rock ranges from 1 to $4 \times 10^{-11} \text{ m}^2 \text{ s}^{-1}$, with the order of phthalate < toluene < adipate < oxalate. These values are one order of magnitude lower than the effective diffusion of HDO. The adjustment of parameters D_e and α was performed using Eq. (7) by adjusting simultaneously both upstream and downstream data. The corresponding best fit values of D_e and α values are gathered in Table 2. The rock capacity factors ($\alpha = R \varepsilon$), sometimes referred as “apparent porosity”, range from 0.47 (phthalate) to 7.72 (oxalate), higher than the total porosity quantified with HDO ($\varepsilon = 0.41$). This data quantifies the retention of the molecules during migration in Tégulines clay rock. The corresponding solid-liquid distribution ratios calculated from Eq. 6 are discussed in the following sections.

Table 2 Reference of diffusion cell experiments, n°1 to 6. Corresponding diffusion parameters adjusted from experimental results (HDO for water tracer). D_0 values are taken from Haynes (2014). *reprocessed to account for the experimental diffusion gradient.

Diffusion cell (Tracer)	IS (M)	D_e (water) ($10^{-10} \text{ m}^2 \text{ s}^{-1}$)	ε (water)	α (org)	D_0 (org) ($10^{-10} \text{ m}^2 \text{ s}^{-1}$)	D_e (org) ($10^{-12} \text{ m}^2 \text{ s}^{-1}$)	Π	R_d^{CELL} (L kg ⁻¹)	R_d^{BATCH} (L kg ⁻¹)
Cell n°1 ³H-phthalate	0.02	1.04 ± 0.05	0.41 ± 0.06	0.47 ± 0.05	6.96	10.05 ± 0.70	0.32 ± 0.03	0.16 ± 0.04	2.33 ± 0.10
Cell n°2 ³H-adipate	0.02	1.43 ± 0.16	0.45 ± 0.06	0.64 ± 0.10	6.39	23.63 ± 2.70	0.58 ± 0.10	0.30 ± 0.08	-
Cell n°3 ¹⁴C-oxalate	0.02	1.65 ± 0.21	0.47 ± 0.08	7.58 ± 1.50	9.87	36.44 ± 4.50	0.52 ± 0.10	5.93 ± 1.22	4.65 ± 0.10
Cell n°4 ¹⁴C-oxalate	0.32 (phthal.)	0.96 ± 0.05	0.34 ± 0.05	5.59 ± 1.20	9.87	23.32 ± 4.70	0.57 ± 0.11	4.31 ± 0.97	-
Cell n°5 ¹⁴C-oxalate	0.32 (NaNO ₃)	1.93 ± 0.23	0.46 ± 0.06	11.12 ± 1.10	9.87	40.84 ± 2.80	0.50 ± 0.07	8.80 ± 0.89	-
Cell n°6 ³H-toluene	0.02	1.30 ± 0.04	0.41 ± 0.05	3.30 ± 0.80	8.50	38.7* ± 3.6	0.82 ± 0.8	2.45 ± 0.65	2.57 ± 0.68

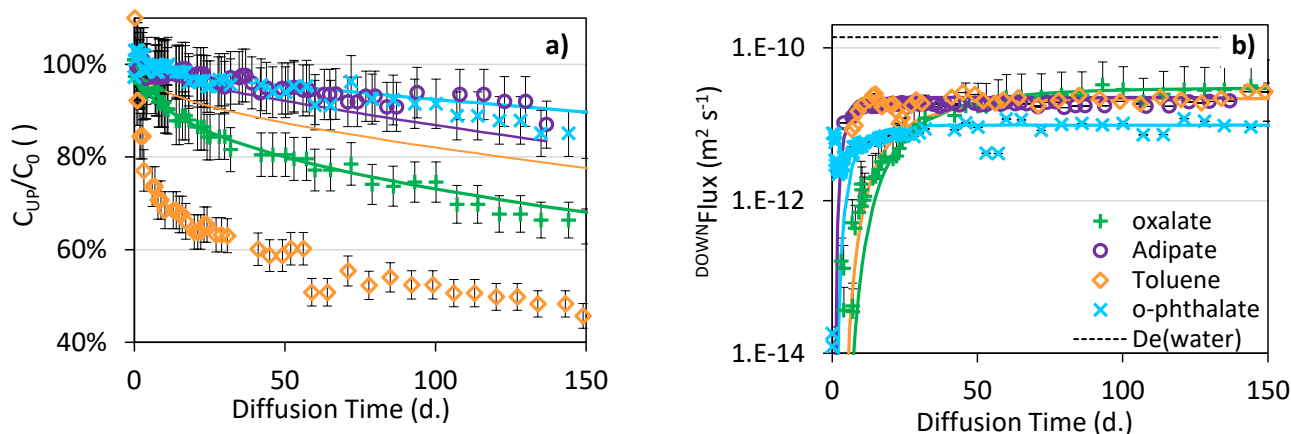


Fig. 2. Diffusion data of organic compounds in Tégulines clay rock.

(a) Upstream concentration (b) Normalized Downstream flux. Solid lines represent best fit modelling (Upstream and downstream data adjusted simultaneously). Dashed line represents the average value measured for water, $D_e(\text{water}) = (1.38 \pm 0.37) \times 10^{-10} \text{ m}^2 \text{ s}^{-1}$.

3.3. Co-diffusion of organic and inorganic solutes

In order to get insights on the various mechanism occurring, e.g. anion exclusion and synergetic or competitive effects, the diffusion of oxalate was measured in presence of organic and inorganic plumes. Additional through-diffusion experiments were performed with ionic strength increased by an order of magnitude, i.e. from $2.33 \cdot 10^{-2} \text{ M}$ in Tégulines pore water, up to $3.2 \cdot 10^{-1} \text{ M}$. Ionic strength ($IS = 0.32 \text{ M}$) was imposed by the presence of 0.1 M sodium phthalate and 0.3 M NaNO_3 respectively. Diffusion data of oxalate under these conditions are provided in Fig. S6. The adjusted parameters, including D_e and α values, are displayed in Table 2. Significant variation of $D_e(\text{oxalate})$ and $\alpha(\text{oxalate})$ values are observed in presence of saline and organic plume. Yet, the difference observed between both experiments at high ionic strength, i.e. o-phthalate and NaNO_3 plume, indicates that ionic strength is not the only parameter affecting migration and anion exclusion. The transitory state during diffusion of oxalate lasted ~ 15 days in raw Tégulines pore water. This transitory state was shorter (10 days) in presence of 0.3 M NaNO_3 , while slightly longer (30 days) with addition of 0.1 M sodium phthalate. Hence, both experiments at high ionic strengths induced opposite disturbances compared to the “sound” state. These effects are quantified more precisely by the effective diffusion coefficients, D_e , which is an indicator of charge or steric exclusion, and rock capacity factor, α , which is an indicator of retention (Table 2). The possible mechanisms occurring, e.g. anion exclusion or pH drift are reviewed in the following section.

Table 3 Solid-liquid distribution coefficients measured by batch experiments on Tégulines clay rock. $\text{pH} = 7.2 \pm 0.2$, $T = 22 \pm 2 \text{ }^\circ\text{C}$. $V/m = 6 / 1.5 \text{ mL g}^{-1}$.

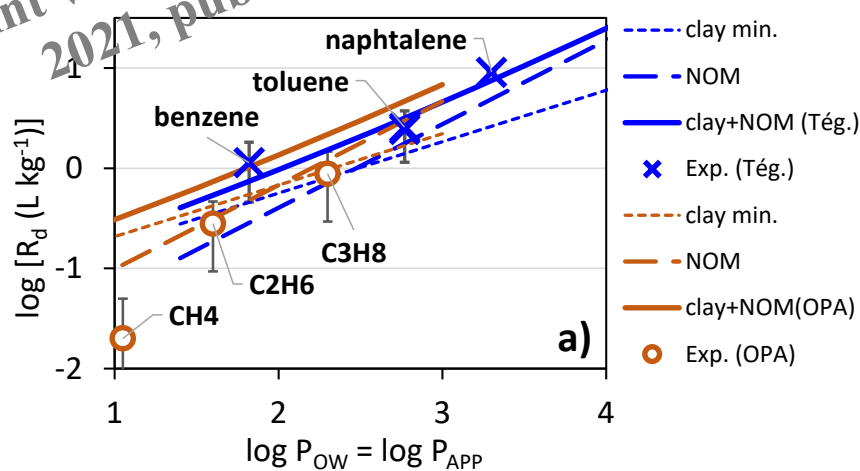
Compound	o-phthalate	Oxalate	benzoate	naphthalene	toluene	benzene
$R_d (\text{L kg}^{-1})$	2.33	4.65	0.55	9.10	2.57	1.14
$\pm u(R_d)$	± 0.10	± 0.10	± 0.23	± 0.23	± 0.68	± 0.18

4. Discussion

4.1 Retention of lipophilic compounds ($\log P_{\text{ow}} > 1$)

The interaction between neutral aromatic compounds and soils is mainly related to absorption mechanism into NOM. Such hypothesis is easily assessed by representing the correlation between

retention and lipophilicity of sorbates (Karickhoff et al., 1979). Lipophilicity of solutes is usually quantified by their octanol/water partition coefficient, P_{OW} . Strong correlations are observed between P_{OW} values and affinity on the NOM fraction of sorbents, i.e. $K_{OC} = R_d/f_{OC}$ (f_{OC} being the mass fraction of organic matter in the sorbent). Such correlation is illustrated in Fig. S7, with the corresponding linear regression $\log K_{OC} \sim 0.84 \times \log P_{OW} + 0.23$ ($R^2 = 0.84$). The value of the slope: +0.84, close to unity, traduces a thermodynamic equilibrium, with similar interactions involved in absorption and partitioning mechanisms, e.g. free enthalpy of solvation. The value $\log K_{OC} = +1.07$ (for $\log P_{OW} = +1$) quantifies a strength of interaction between slightly lipophilic solutes and NOM. On the other hand, the affinity between clay minerals and organic solutes is also well documented (Barré et al., 2014) and similar correlations due to hydrophobic interactions are expected (Willemsen et al., 2019). Yet, the correlations between retention and $\log P_{OW}$ are less obvious, as illustrated in Fig. S7, with $\log K_{CM} \sim 0.51 \times \log P_{OW} - 0.98$. The low correlation ($R^2 = 0.11$) and strong data disparity are caused by the diversity of phyllosilicates structures, as well as various adsorption mechanisms (Barré et al., 2014). Still, the value $\log K_{CM} = -0.47$ (for $\log P_{OW} = +1$) indicates an affinity of clay minerals, almost two orders of magnitude below the previous value for NOM. Hence, the two previous correlations are useful to assess, in a first macroscopic approach, the respective contributions of NOM and clay minerals to the retention in sedimentary rocks. Fig. 3 (a) illustrates the relative contributions of absorption in NOM and of adsorption on clay minerals in two examples of sedimentary rocks. The agreement between predicted values and experimental data on Tégulines ($f_{OC} \sim 0.5\%$, $f_{CM} \sim 50\%$) and OPA ($f_{OC} \sim 0.8\%$, $f_{CM} \sim 60\%$) clay rocks is rather good. The fact that clay minerals contribution displays a lower slope than NOM contribution induces interesting features. The contribution of absorption mechanism in NOM prevails for high values of $\log P_{OW}$. This remains true even in sedimentary rocks with low NOM content, such as Tégulines clay rock ($f_{OC} = 0.5\%$, Lerouge et al., 2018), OPA clay ($f_{OC} = 0.5\%$, Wersin et al., 2008), or COx clay rock ($f_{OC} = 0.6\%$, Gaucher et al., 2004). On the other hand, the adsorption on phyllosilicates may control the retention of solutes with low $\log P_{OW}$ values, especially for such rocks with high contents of clay minerals ($f_{CM} > 50\%$). Further investigations still are necessary to assess such assumption. As a corollary, the accurate measurement of low NOM content ($f_{OC} < 1\%$) provides a useful data, complementary to clay mineralogy. This allows to determine sorbing phases and predict the migration of lipophilic compounds (dissolved gas, pesticides, etc.) in sedimentary rocks and geobarriers.



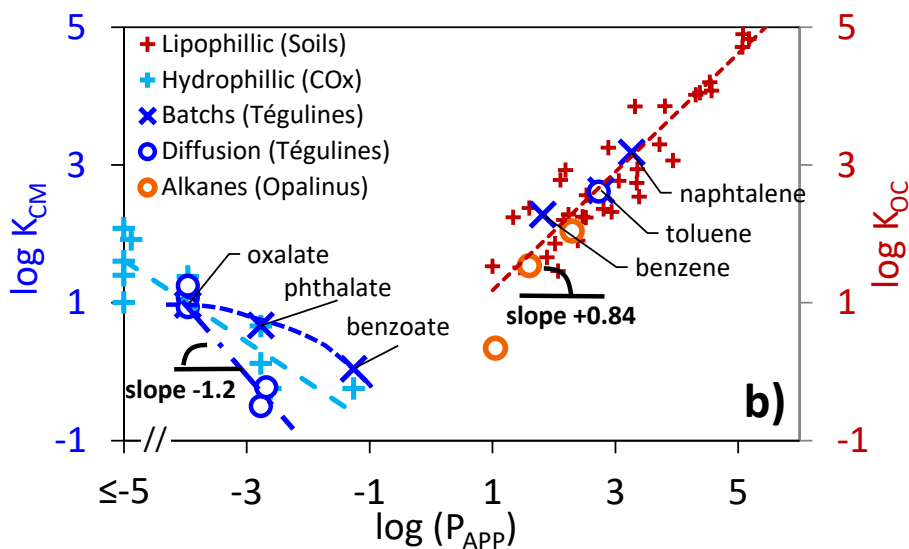


Fig. 3. Correlation between partition coefficient of organic compounds and their retention properties in natural media (near neutral pH ~7.2).

a) Data for lipophilic compounds ($\log P_{APP} > 1$) measured on Tégulines (Tég.) and Opalinus (OPA) clay rocks. Dashed lines: theoretical contribution expected from absorption in NOM and adsorption on phyllosilicates. Signs correspond to experimental data: Adsorption and through-diffusion in Tégulines at $22 \pm 2^\circ\text{C}$ (This work), In situ out-diffusion experiment in OPA at $16.5 \pm 1.5^\circ\text{C}$ (Vinsot *et al.*, 2017).

b) Comparison of adsorption data for hydrophilic compounds ($K_{CM} = R_d/f_{CM}$) and absorption data of lipophilic compounds ($K_{OC} = R_d/f_{OC}$). Data on Tégulines (This work), OPA (Vinsot *et al.*, 2017), COx clay rock (Rasamimanana *et al.*, 2017a) and soils (Karickhoff *et al.*, 1981).

4.2 Retention of hydrophilic compounds ($\log P_{APP} < -1$)

Ionizable compounds are among the most widespread hydrophilic compounds. For carboxylates (RCOO^-), octanol/water apparent partition coefficient may be estimated from the value of carboxylic acids (RCOOH) using the Eq. 8 (Sangster, 1989):

$$P_{APP} = \frac{P_{OW}}{1 + 10^{(\text{pH} - \text{p}K_{a1})}} \quad (8)$$

However, such equation becomes unsuitable for highly hydrophilic compounds. For that reason, $\log P_{APP}$ values were experimentally measured in this study. The methodology and results are provided in supplementary material (Fig. S1). The corresponding values are gathered in Table 1. As for hydrophilic compounds, a correlation is observed between $\log R_d$ and $\log P_{APP}$ values of ionizable compounds (Fig. 3, b). In this case, the slope is negative, which indicates a retention mechanism differing from that for aromatic compounds, i.e. more likely an adsorption mechanism on surfaces of clayey minerals. Hence, R_d values are normalized by the content of clay minerals in the media, $K_{CM} = R_d/f_{CM}$, in order to ease the comparison between rocks. Results on Tégulines soft clay rock (Fig. 3, b) are in line with data previously published on COx hard clay rock (Chen *et al.*, 2018; Durce *et al.*, 2015; Rasamimanana *et al.*, 2017b). A linear correlation is observed between retention of solutes and hydrophilicity of sorbates and that solvation and retention mechanism involve similar interactions. Moreover, the value of the slope close to unity, (-1.2 ± 0.1) , tends to indicate that thermodynamic equilibrium is reached during diffusion experiments. Some correlation between hydrophilicity of ionizable sorbates and retention has been previously reported on COx clay rock, but without evidence of any sorption “maximum” (Rasamimanana *et al.*, 2017a). The correlation observed on Tégulines clay

rock, $K_{CM} = f(\log P_{APP})$, points out a rise to a plateau for highly hydrophilic sorbates, e.g. oxalate. This means that below a certain value of $\log P_{APP}$, the affinity between hydrophilic sorbates and minerals does not increase “indefinitely”. This trend differs from the affinity of lipophilic compounds which increases up to $\log P_{OW}$ values over +6.

Speciation calculation are illustrated in supplementary material (Fig. S8). Data indicates that the acidic form of solutes becomes negligible at near-neutral pH. Hence, the retention mechanism may imply anionic species, rather than protonated organic acids. On the other hand, the relative contribution of mineralogical phases (especially clay minerals and oxides) to the retention of ionizable compounds deserves further numerical or experimental investigations (Ilina et al., 2020). For example, the presence of oxidized minerals in samples may contribute to differences between batch and diffusion experiments, as observed for *o*-phthalate and discussed furtherly.

4.3. Diffusion data and exclusion from rock porosity

The effective diffusion coefficients obtained from the diffusion experiments are lower than that of water, almost by an order of magnitude (Table 2). This behaviour is usually explained by a phenomenon of anion exclusion in surface charged media (de Haan, 1968). Such data can be discussed using the exclusion factor, Π , defined by Eq. 9:

$$\Pi(\text{solute}) = \frac{D_e(\text{solute})/D_e(\text{water})}{D_0(\text{solute})/D_0(\text{water})} \quad (9)$$

where D_e is the effective diffusion coefficient in the porous solid and D_0 in water. The ratio $D_e(\text{solute})/D_e(\text{water})$ quantifies the effect of clay rock on the diffusion of a solute, in comparison with non-reactive species such as water. This ratio is then normalized by $D_0(\text{solute})/D_0(\text{water})$, in order to remove the contribution of solvent (poral water) on the diffusivity. Thus, the exclusion factor Π isolates the effect from the porosity of the media (i.e. tortuosity and constrictivity, Van Brakel and Heertjes, 1974) on the diffusion pathways of solutes. Fig. 4 shows the exclusion factor of anionic solutes as a function of their sizes (estimated from molecular mass). Data is reported for both COx and Tégulines clay rocks. Previous studies evidenced anion exclusion in COx clay rock for both inorganic (Descostes et al., 2008) and organic anions (Dagnelie et al., 2018), with exclusion factors down to 0.1 (i.e. $\Pi(\text{anion}) \ll \Pi(\text{water}) = 1$). This phenomena is usually explained by the presence of surface charged clay minerals (Tournassat et al., 2016) and more pronounced when pore size is small (Gaboreau, et al., 2016; Wigger et al., 2018). For example, a strong anion exclusion is observed in COx clay units, quantified with $\Pi(\text{Cl}^-/\text{COx}) \sim 0.3 \pm 0.1$ (Descostes et al., 2008). In contrast, no anion exclusion was evidenced with chloride in Tégulines soft clay rock, despite similar content in clay minerals. The absence of chloride exclusion in Tégulines, $\Pi(\text{Cl}^-/\text{Tégulines}) \sim 1$, can be explained by the shallow depth of the media: -75 m to -10 m (Debure et al., 2018). This leads to a less dense material ($\rho^{\text{dry}} \sim 1.7 \text{ g cm}^{-3}$), and a limited diagenetic processes with pore diameters mainly higher than 30–50 nm (Lerouge et al., 2018).

Surprisingly, a significant exclusion was observed for organic molecules in Tégulines clay rock, thus differing from chloride case (Fig. 4, a). Regarding exclusion from porosity, the size of diffusing solutes may also decrease exclusion factor by steric effect, as clearly evidenced with neutral species, $\Pi(\text{toluene}/\text{Tégulines}) \sim 0.82 \pm 0.08$. The values for adipate and oxalate, $\Pi \sim 0.5 \pm 0.1$, are even lower than that of toluene (despite similar mass), indicating an additional contribution of charge to the exclusion from porosity. Still, the value of $\Pi(\text{organic anions})$ mainly decreases with the size of solutes (Fig. 4) for both Tégulines and COx clay rock. These trends indicate that the exclusion factors of complex anions is highly related to their sizes as compared to the size of pores in the media. Hard COx rock, with a pore size $\sim 6\text{-}8 \text{ nm}$, displays a strong anion exclusion, even for chloride. Only small inorganic anion, such as Cl^- , display little exclusion factor in soft Tégulines rock (pore size $\sim 20\text{-}30 \text{ nm}$).

Since a significant exclusion is observed for larger species in both soft and hard rocks, other anions than Cl^- should be preferred to quantify exclusion factor of environmental media, e.g. NO_3^- , SO_4^{2-} . These references, if conservative in the media, should be more representative of other contaminants such as AsO_4^{3-} or SeO_4^{2-} .

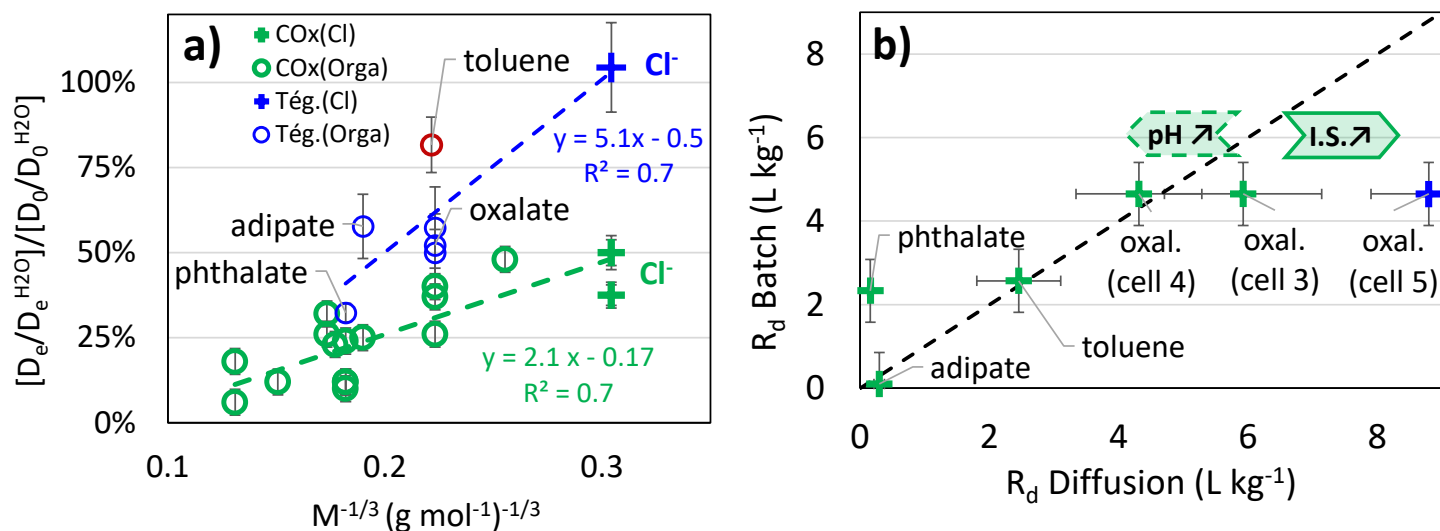


Fig. 4. Diffusion data for organic solutes. a) Exclusion factor for organic anions in COx clay rock (Dagnelie et al., 2014, 2018) and in Téglines clay rock (Tégl.) (This work).

M: molecular mass. b) Solid-liquid distribution coefficient, R_d (L kg^{-1}), measured in Téglines by batch experiments (X axis) and diffusion experiments (Y axis).

4.4. Retardation and environmental implications

Assessing the environmental impact of hazardous materials requires the estimation of their migration properties, such as sorption, retardation and diffusivity. The predictive migration modelling in natural media requires several building blocks. This includes accurate description of the media, sorbing phases, and understanding of retention processes. It is then useful to assess retention by various methodologies, e.g. molecular simulations, batch experiments, migration experiments. This approach strengthens the description on underlying phenomena and the accuracy on corresponding data. Such comparison of results is provided in Fig. 3 (b). A large discrepancy is quantified between batch and diffusion data for slightly lipophilic compounds, i.e. $-4 < \log P_{\text{APP}} < 0$, similarly to previous data on COx clay rock (Dagnelie et al., 2018) or compacted clay minerals (Chen et al., 2018). This discrepancy is especially striking for o-phthalate, for which diffusion data suggests strong steric and charge exclusion (Fig. 4). Similar observations on COx clay rock and illite suggest a “collapse” of retardation when exclusion factor decreases below a “threshold” value. Yet, the mechanism leading to such discrepancy is unclear. Further investigations are required to assess eventual hypotheses, e.g. effect of anion exclusion on surface accessibility, oxidative perturbation of sulphide minerals in crushed samples leading to additional (hydroxy)oxides, kinetic effects, etc. Meanwhile, diffusion experiments and especially long-term *in situ* experiments seem mandatory in order to accurately quantify the retardation factor of such solutes.

The batch and diffusion experiments provided consistent data for both toluene ($\log P_{\text{APP}} = 2.73$, lipophilic) and oxalate ($\log P_{\text{APP}} = -3.96$, hydrophilic). This validates the reactive transport model, despite simplistic hypothesis (reversible and instantaneous retention) and the absence of speciation

calculations. The good agreement between results from both types of experiments strengthens the accuracy on corresponding values: R_d (toluene/Tégulines) $\sim 2.5 \pm 0.3 \text{ L kg}^{-1}$ and R_d (oxalate/Tégulines) $\sim 4.5 \pm 0.5 \text{ L kg}^{-1}$. Given the relatively good accuracy on oxalate retention data, this later compounds was chosen for further co-diffusion experiments. In the case of pollution events, the concomitant release of various contaminants leads to co-sorption and co-diffusion phenomena. Several mechanisms may affect retention: competitive sorption, pH drift, modification of IS, etc. In this context, diffusion of oxalate was performed in presence of 0.1 M of o-phthalate (diffusion cell n°4) or 0.3 M of NaNO_3 (diffusion cell n°5). The retention of oxalate in sound sample (cell n°3), in presence of phthalate (cell n°4), and in batch experiments, are in agreement with regard to the uncertainties. This demonstrates that eventual pH drifts (between 7 and 9) due to the presence of organic plume (Fralova et al., 2021) do not affect significantly diffusion. On contrary, a slight increase of R_d (oxalate) is observed in presence of NaNO_3 . This result may be linked to the effect of ionic strength, which decreases anion exclusion, and thus increases accessibility to surfaces and retardation. It is interesting to note that such an effect was not observed in cell 4, despite a similar ionic strength. This may probably be due to the diffusion speed of the perturbation compared to oxalate diffusion. The effective diffusion coefficient of o-phthalate is lower than that of oxalate. Thus in cell 4, the phthalate plume might diffuse too “slowly” to affect significantly the diffusion of oxalate. Whereas in cell 5, the effective diffusion of NO_3^- , which is faster than oxalate (Dagnelie et al., 2017), leads to an increase of IS along the pathway of oxalate. Such effect may be responsible of the decrease of anion exclusion and eventual increase of retention. This also confirms that oxalate exclusion is partially induced by charge effects (in addition to steric effects), which is in agreement with measured exclusion factors (i.e. $\Pi(\text{oxalate}) < \Pi(\text{toluene})$, Fig. 4). Overall, these results illustrate the various mechanisms, with eventual antagonistic effects, which may arise from release of complex saline and organic plumes during pollution events.

Conclusion

Retention and diffusion of various organic compounds were quantified in the Tégulines soft clay rock. A comparison is made with previous data measured on COx hard clay rock. A significant affinity with clay rich rocks was observed for both lipophilic ($\log P_{\text{OW}} > 1$) and hydrophilic ($\log P_{\text{APP}} < -1$) compounds. Neutral aromatic compounds mainly undergo absorption mechanism in NOM. Such absorption is well correlated with the content of NOM in the sorbent and the lipophilicity of the sorbate. The organic phase remains the main sorbent for such compounds, even in media with low organic content, $f_{\text{OC}} \leq 0.6\%$. Still, clay minerals may contribute to the retention of low lipophilicity compounds in such clay-rich rocks ($f_{\text{CM}} \geq 40\%$). More generally, the retention measured on crushed clay rock accurately predicts retardation measured by diffusion experiments. Additional mechanism of intraparticulate diffusion should eventually be taken into account for migration modelling.

The ionizable compounds displayed values of solid-liquid distribution coefficients similar to neutral compounds, but mainly due to adsorption mechanism. Surprisingly, this adsorption was also correlated with the lipophilicity of solutes, with a maximum affinity reached when $\log P_{\text{APP}} \leq -4$. The diffusion data evidences an exclusion from rock porosity, with a contribution of both size and charge of solutes. Such exclusion is higher for large organic anions than for “small” inorganic anions such as chloride. The size of solutes should then be taken into account for selection of reference conservative tracers or environmental assessment. The diffusive retardation of solutes with intermediate polarities ($\log P_{\text{APP}} \sim -2$), such as o-phthalate, was lower than expected from batch experiments. Further studies, such as field experiments, would be interesting in order to quantify these values and the relative contribution of clay minerals and (hydroxy)oxides on the retention mechanisms.

Acknowledgments

This work was financed by CEA and the French radioactive waste management agency (Andra).

References

- Altmann, S., Tournassat, C., Goutelard, F., Parneix, J.C., Gimmi, T., Maes, N., 2012. Diffusion-driven transport in clayrock formations. *Appl. Geochemistry* 27, 463–478.
- Andra, 2015. Projet de stockage des déchets radioactifs de faible activité massique à vie longue (FAVL) – Rapport d'étape 2015. FRPADPG150010.
- Amédéo, F., Matrimon, B., Deconinck, J.-F., Huret, E., Landrein, P., 2017. Les forages de Juzanvigny (Aube, France): litho-biostratigraphie des formations du Barrémien à l'Albien moyen dans l'est du bassin de Paris et datations par les ammonites. *Geodiversitas* 39, 185–212.
- Appelo, C.A.J., Van Loon, L.R., Wersin, P. 2010. Multicomponent diffusion of a suite of tracers (HTO, Cl, Br, I, Na, Sr, Cs) in a single sample of Opalinus Clay. *Geochim. Cosmochim. Acta* 74, 1201–1219.
- Barré, P., Fernandez-Ugalde, O., Virto, I., Velde, B., Chenu, C. 2014. Impact of phyllosilicate mineralogy on organic carbon stabilization in soils: incomplete knowledge and exciting prospects. *Geoderma* 235–236, 382–395.
- Borisover, M.D., Graber, E.R., 1997. Specific interactions of organic compounds with soil organic carbon. *ACS Div. Environ. Chem. Prepr.* 37, 172–174.
- Borisover, M., Davis, J.A., 2015. Adsorption of Inorganic and Organic Solutes by Clay Minerals. *Dev. Clay Sci.* 6, 33–70.
- Van Brakel, J., Heertjes, P.M., 1974. Analysis of Diffusion in Macroporous Media in Terms of a Porosity, a Tortuosity and a Constrictivity Factor. *International Journal of Heat and Mass Transfer* 17 (9), 1093–1103.
- Chen, Y., Glaus, M.A., Van Loon, L.R., Mäder, U., 2018. Transport of Low Molecular Weight Organic Compounds in Compacted Illite and Kaolinite. *Chemosphere* 198, 226–37.
- Crank, J. 1975. *The Mathematics of Diffusion*. London: Clarendon Press.
- Dagnelie, R.V.H., Descostes, M., Pointeau, I., Klein, J., Grenut, B., Radwan, J., Lebeau, D., Georgin, D., Giffaut, E., 2014. Sorption and diffusion of organic acids through clayrock: comparison with inorganic anions. *J. Hydrol.* 511, 619–627.
- Dagnelie, R.V.H., Arnoux, P., Enaux, J., Radwan, J., Nerfie, P., Page, J., Coelho, D., Robinet, J.-C., 2017. Perturbation induced by a nitrate plume on diffusion of solutes in a large-scale clay rock sample. *Appl. Clay Sci.* 141, 219–226.
- Dagnelie, R.V.H., Rasamimanana, S., Blin, V., Radwan, J., Thory, E., Robinet, J.-C., Lefèvre, G., 2018. Diffusion of Organic Anions in Clay-Rich Media: Retardation and Effect of Anion Exclusion. *Chemosphere* 213, 472–80.
- Debure, M., Tournassat, C., Lerouge, C., Madé, B., Robinet, J.-C., Fernández, A.M., Grangeon, S., 2018. Retention of Arsenic, Chromium and Boron on an Outcropping Clay-Rich Rock Formation (the Tégulines Clay, Eastern France). *Sci.Total Environ.* 642, 216–29.
- Descostes, M., Blin, V., Bazer-Bachi, F., Meier, P., Grenut, B., Radwan, J., Schlegel, M.L., Buschaert, S., Coelho, D., Tevissen, E., 2008. Diffusion of Anionic Species in Callovo-Oxfordian Argillites and Oxfordian Limestones (Meuse/Haute-Marne, France). *Appl. Geochem.* 23, 655–77.
- Durce, D., Bruggeman, C., Maes, N., Van Ravestyn, L., Brabants, G. 2015. Partitioning of organic matter in Boom Clay: Leachable vs mobile organic matter. *Appl. Geochem.* 63, 69–181.
- Fralova, L., Lefèvre, G., Madé, B., Marsac, R., Thory, E., Dagnelie, R.V.H. Effect of organic compounds on the retention of radionuclides in clay rocks: Mechanisms and specificities of Eu(III), Th(IV), and U(VI). *Appl. Geochem.* 104859, 2021.

Gaboreau, S., Robinet, J.-C., Prêt. D. 2016. Optimization of Pore-Network Characterization of a Compacted Clay Material by TEM and FIB/SEM Imaging. *Microporous and Mesoporous Mater.* 224, 116–128.

Gaucher, E., Robelin, C., Matray, J.-M., Négrel, G., Gros, Y., Heitz, J.F., Vinsot, A., Rebours, H., Cassagnabère, A., Bouchet, A., 2004. ANDRA underground research laboratory: interpretation of the mineralogical and geochemical data acquired in the Callovian–Oxfordian formation by investigative drilling. *Phys. Chem. Earth*, 29, 55–77.

Gu, B., Schmitt, J., Chen, Z., Liang, L., McCarthy, J.F., 1994. Adsorption and Desorption of Natural Organic Matter on Iron Oxide: Mechanisms and Models. *Environ. Sci. Technol.* 28, 38–46.

de Haan, F.A.M., 1968. The Negative Adsorption of Anions (Anion Exclusion) in Systems with Interacting Double Layers. *J. Phys. Chem.* 68 (10), 2970–2977.

Hansch, C., Leo, A., Hoekman, D., 1995. Exploring QSAR. Hydrophobic, electronic, and steric constants. ACS Professional Reference Book. ACS, Washington.

Haynes, W.M. (Ed.), 2014. CRC Handbook of Chemistry and Physics, 95th Edition, CRC Handbook of Chemistry and Physics, 95th Edition. CRC press.

Hwang, Y.S., Liu, J., Lenhart, J.J., Hadad. C.M., 2007. Surface Complexes of Phthalic Acid at the Hematite/Water Interface. *J. Colloid Interface Sci.* 307 (1), 124–34.

Iliina, S.M., Maran, L., Lourino-Cabana, B., Eyrolle, F., Boyer, P., Coppin, F., Sivry, Y., Gélabert, A., Johnson, S.B., Yoon, T.H., Slowey, A.J., Brown, G.E., 2004. Adsorption of organic matter at mineral/water interfaces: 3. Implications of surface dissolution for adsorption of oxalate. *Langmuir* 20, 11480–11492.

Kang, S., Xing, B., 2007. Adsorption of Dicarboxylic Acids by Clay Minerals as Examined by in Situ ATR-FTIR and Ex Situ DRIFT. *Langmuir* 23 (13), 7024–31.

Karickhoff, S.W., Brown, D.S., Scott. T.A., 1979. Sorption of Hydrophobic Pollutants on Natural Sediments. *Water Research* 13 (3), 241–48.

Karickhoff, S.W., 1981. Semi-empirical estimation of sorption of hydrophobic pollutants on natural sediments and soils. *Chemosphere*, 10 (8), 833–846.

Karnitz, O., Gurgel, L.V.A., de Melo, J.C.P., Botaro, V.R., Melo, T.M.S., de Freitas Gil, R.P., Gil, L.F., 2007. Adsorption of heavy metal ion from aqueous single metal solution by chemically modified sugarcane bagasse. *Bioresour. Technol.* 98, 1291–1297.

Lerouge, C., Robinet, J.C., Debure, M., Tournassat, C., Bouchet, A., Fernández, A.M., Flehoc, C., Lerouge, C., Debure, M., Henry, B., Fernandez, A. M., Blessing, M., Proust, E., Madé, B., Robinet, J. C. 2020. Origin of dissolved gas (CO₂, O₂, N₂, alkanes) in pore waters of a clay formation in the critical zone (Tégulines Clay, France). *Appl. Geochem.* 104573.

Maes, N., Bruggeman, C., Govaerts, J., Martens, E., Salah, S., Van Gompel, M. 2011. A consistent phenomenological model for natural organic matter linked migration of Tc(IV), Cm(III), Np(IV), Pu(III/IV) and Pa(V) in the Boom Clay. *Phys. Chem. Earth* 36, 1590–1599.

Melkior, T., Yahiaoui, S., Thoby, D., Motellier, S., Barthès, V., 2007. Diffusion coefficients of alkaline cations in Bure mudrock. *Phys. Chem. Earth* 32, 453–462.

Missana, T., Colàs, E., Grandia, F., Olmeda, J., Mingarro, M., García-Gutiérrez, M., Munier, I., Robinet, J.C., Grivé, M., 2017. Sorption of radium onto early cretaceous clays (Gault and Plicatules Fm). Implications for a repository of low-level, long-lived radioactive waste. *Appl. Geochemistry* 86, 36–48.

Pageot, J., Rouzaud, J.N., Gosmain, L., Deldicque, D., Comte, J., Ammar, M.R., 2016. Nanostructural characterizations of graphite waste from French gas-cooled nuclear reactors and links with 14C inventory. *Carbon N. Y.* 105, 77–89.

Pageot, J., Rouzaud, J.N., Gosmain, L., Duhart-Barone, A., Comte, J., Deldicque, D., 2018. 14C selective extraction from French graphite nuclear waste by CO₂ gasification. *Progress in Nuclear Energy*, 105, 279–286.

- Pignatello, J.J., Xing, B., 1996. Mechanisms of slow sorption of organic chemicals to natural particles. *Environ. Sci. Technol.* 30 (1), 1–11.
- Pinsuwan, S., Li, A., Yalkowsky, S.H., 1995. Correlation of Octanol/Water Solubility Ratios and Partition Coefficients. *J. Chem. Eng. Data* 40, 623–626.
- Poncet, B., Petit, L., 2013. Method to assess the radionuclide inventory of irradiated graphite waste from gas-cooled reactors. *J. Radioanal. Nucl. Chem.* 298, 941–953.
- Rasamimanana, S., Lefèvre, G., Dagnelie, R.V.H., 2017a. Adsorption of Polar Organic Molecules on Sediments: Case-Study on Callovian-Oxfordian Claystone. *Chemosphere* 181, 296–303.
- Rasamimanana, S., Lefèvre, G., Dagnelie, R.V.H., 2017b. Various Causes behind the Desorption Hysteresis of Carboxylic Acids on Mudstones. *Chemosphere* 168, 559–67.
- Sangster, J., 1989. Octanol-water partition coefficient of simple organic compounds. *J. Phys. Chem. Ref. Data* 18 (3), 1111–1227.
- Sarazin, G., Michard, G., Prevot F., 1999. A rapid and accurate spectroscopic method for alkalinity measurements in sea water samples. *Water Res.* 33 (1), 290–294.
- Savoie, S., Frasca, B., Grenut, B., Fayette, A., 2012. How mobile is iodide in the Callovo-Oxfordian claystones under experimental conditions close to the in situ ones? *J. Contam. Hydrol.* 142–143, 82–92.
- Schaffer, M., Licha, T., 2015. A framework for assessing the retardation of organic molecules in groundwater: Implications of the species distribution for the sorption-influenced transport. *Sci. Total Environ.* 524–525, 187–194.
- Shackelford, C.D., Moore, S.M., 2013. Fickian diffusion of radionuclides for engineered containment barriers: Diffusion coefficients, Porosities, And complicating issues. *Eng. Geol.* 152, 133–147.
- Tournassat, C., Gaboreau, S., Robinet, J.-C., Bourg, I.C., Steefel, C.I., 2016. Impact of microstructure on anion exclusion in compacted clay media. *The Clay Minerals Society Workshop Lectures Series*, 21 (11), 137–149.
- Vinsot, A., Anthony, C., Appelo, J., Lundy, M., Wechner, S., Cailteau-Fischbach, C., de Donato, P., Pironon, J., Lettry, Y., Lerouge, C., De Cannière, P. 2017. Natural Gas Extraction and Artificial Gas Injection Experiments in Opalinus Clay, Mont Terri Rock Laboratory (Switzerland). *Swiss Journal of Geosciences* 110 (1), 375–90.
- Wersin, P., Soler, J.M., Van Loon, L., Eikenberg, J., Baeyens, B., Grolimund, D., Gimmi, T., Dewonck, S., 2008. Diffusion of HTO, Br⁻, I⁻, Cs⁺, 85Sr²⁺ and 60Co²⁺ in a clay formation: Results and modelling from an in situ experiment in Opalinus Clay. *Applied Geochem.* 23, 4, 678–691.
- Wigger, C., Gimmi, T., Muller, A., Van Loon, LR. 2018. The Influence of Small Pores on the Anion Transport Properties of Natural Argillaceous Rocks – A Pore Size Distribution Investigation of Opalinus Clay and Helvetic Marl. *Appl. Clay Sci.* 156, 134–143.
- Willemsen, J.A.R., Myneni, S.C.B., Bourg, I.C. 2019. Molecular dynamics simulations of the adsorption of phthalate esters on smectite clay surfaces. *J. Phys. Chem. C*, 123, 13624–13636.

Supplementary Material for:

Mobility of organic compounds in a soft clay-rich rock

(Tégulines clay, France)

Ning Guo^a, Z. Disdier^a, E. Thory^a,

Jean-Charles Robinet^b, Romain V.H. Dagnelie^{a*}

(a) Université Paris-Saclay, CEA, Service d'Étude du Comportement des Radionucléides,

91191, Gif-sur-Yvette, France

(b) Andra, R&D Division, parc de la Croix Blanche, 92298, Châtenay-Malabry, France

Table S1. Mineralogical composition of clay rock samples

Sample		AUB01919	AUB01826
		AUB1011	AUB1010
Depth (m)		-20.4	-22.03
Clay minerals	Mica+Ill.+Glaucinite	24.2	22.4
	I/S R=0	15.8	14.6
	Kaolinite	13.1	9.7
	Chlorite	1.4	1.2
	Pyrophyllite	0	0
	% Clay minerals	54.5	47.9
Carbonates	Calcite	3.6	4.4
	Dolomite / Ankerite	1.4	1.6
	% Carbonates	5	6
Tectosilicates	Quartz	32.5	38.9
	Feldsp.K	3.6	3.7
	Plagioclases	0	0

	% Tectosilicates	36.1	42.6
Others	Pyrite	0.8	0.6
	Sidérite / Hématite / Fe-mx	2.8	2.1
	TiO ₂	0.7	0.7
	Ap/Collo	0.1	0.1
	Gypse	0.1	0
CEC	(meq/100g)	15.4	13.9

Table S2. Metrology of clay rock sample disks used in diffusion experiments

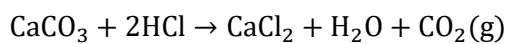
Diffusion Cell	Experiment	Clay Ref.	Mass (g)	Diameter (mm)	Thickness (mm)	$\rho_{\text{saturated}}$ (g/cm³)
1	o-phthalate	AUB1918-01	23.91 ± 0.48	38.03 ± 0.23	11.12 ± 0.09	1.89 ± 0.05
2	Adipate	AUB1918-03	23.50 ± 0.47	37.50 ± 0.45	11.25 ± 0.41	1.89 ± 0.09
3	Oxalte	AUB1918-05	24.21 ± 0.48	38.01 ± 0.02	10.63 ± 0.13	2.01 ± 0.05
4	Oxalate	AUB1918-06	19.54 ± 0.39	34.77 ± 0.18	10.99 ± 0.21	1.87 ± 0.06
5	Oxalate	AUB1918-07	19.88 ± 0.40	33.83 ± 0.10	11.27 ± 0.09	1.96 ± 0.04
6	Toluene	AUB1918-08	26.05 ± 0.52	37.82 ± 0.31	10.93 ± 0.05	2.12 ± 0.06
7	HDO only	AUB1918-09	22.51 ± 0.45	36.06 ± 0.09	11.26 ± 0.27	1.96 ± 0.06
8	HDO only	AUB1918-10	33.24 ± 0.66	37.74 ± 0.13	14.35 ± 0.28	2.07 ± 0.06
9	HDO only	AUB1918-11	22.20 ± 0.44	37.11 ± 0.04	10.14 ± 0.11	2.02 ± 0.05
10	HDO only	AUB1918-12	25.37 ± 0.60	39.68 ± 0.29	10.15 ± 0.34	2.02 ± 0.08
		Average				1.98 ± 0.10

The specific surface area (SSA) was measured by ethylene glycol monoethyl ether (EGME) technique (Heilman et al., 1965). Similar procedure was performed as the measurement of porosity except that EGME was filled in the bottom of the desiccator instead of saturated K₂SO₄ solution. Therefore, the SSA_{EGME} (m²/g) can be obtained by the equation:

$$SSA = \frac{m_{\text{EGME}_{\text{ad}}}}{2.86E-4 \times m_{\text{dry_rock}}} = \frac{m_{\text{wet_rock}} - m_{\text{dry_rock}}}{2.86E-4 \times m_{\text{dry_rock}}} \quad (\text{S1})$$

with $m_{\text{EGME}_{\text{ad}}}$, the mass of EGME absorbed to the clay (g); $m_{\text{wet_rock}}$, the mass of sample after saturated with EGME (g); $m_{\text{dry_rock}}$ is the final mass of sample over-dried after 24 h (g); and $2.86 \cdot 10^{-4}$ g/m² is the mass of EGME absorbed by 1 m² clay (Heilman et al., 1965). The SSA_{EGME} of both AUB01825/15-002-B and AUB01918/15-002-A are 66.9 ± 1.0 and 64.2 ± 0.6 m²/g respectively.

The proportion of carbonate contents was analyzed by Bernard Calcimetry method, which aims at acquiring the carbonate content through measuring the CO₂ volume generated by the reaction between hydrogen chloride acid (HCl) and calcium carbonate (CaCO₃) in the sample:



Thus, the proportion of carbonate can be calculated:


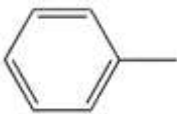

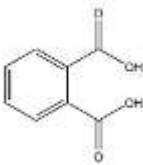
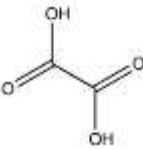
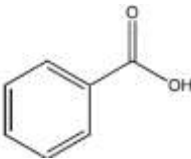

$$\% \text{CaCO}_3 = \frac{V_{\text{measure}}/224}{m} \times 100 \quad (\text{S2})$$

where V_{measure} (mL) is the volume of CO_2 generated by m g sample, 224 mL is the CO_2 volume generated by 1 g CaCO_3 . The carbonate content of both AUB01825/15-002-B and AUB01918/15-002-A are $3.8 \pm 0.3\%$ and $3.9 \pm 0.3\%$ respectively.

Table S3. Composition of synthetic water for Gault.
Mass of salts used for preparation of 5 L of synthetic pore water.

Salts	m_{theo} (g)	Ions	$C_{\text{THEOR.}}$ (mM)	$C_{\text{EXP.}}$ (mM)	Δ (%)
NaHCO₃	1.021	Na⁺	2.43	3.26 ± 0.07	34
KHCO₃	0.335	K⁺	0.67	0.74 ± 0.01	10
CaSO₄	2.069	Ca²⁺	3.09	2.24 ± 0.02	-27
		Mg²⁺	1.94	1.87 ± 0.02	-3
SrCl₂·6H₂O	0.333	Sr²⁺	0.25	0.16 ± 0.00	-36
MgCl₂·6H₂O	0.539	Cl⁻	1.56	1.64 ± 0.11	5
MgSO₄	0.843	SO₄²⁻	4.44	4.39 ± 0.08	1
		HCO₃	3.16	2.27 ± 0.19	-28
		Σ⁺	12.1	10.5 ± 0.08	-13
		Σ⁻	11.2	10.7 ± 0.23	-4
		I.S.	23.3	21.3 ± 0.24	-9

Table S4. Properties of radioactive organic tracers purchased form ARC / Isobio.
Activity and concentration of injection solutions.

Compound	Structure	Labelling	Activity (Bq mL ⁻¹)	C (mol L ⁻¹)
Naphthalene		³ H	3.70E+07	2.50E-05
Toluene		³ H	3.70E+04	9.44
Benzene		¹⁴ C	3.38E+04	11.22
Phthalic acid		³ H	3.70E+07	1.67E-05
Oxalic acid		¹⁴ C	6.14E+05	2.34E-03
Benzoic acid		³ H	3.70E+07	5.00E-05
Adipic acid		³ H	3.70E+07	1.0E-06

Theoretical partition coefficients:

The partition coefficients of organic acids are usually defined for the acidic form: $P_{OW}(A) = C_O(A)/C_W(A)$. Such value is accurate if $pH \ll pK_a$ and HA remains the predominant species in water, i.e. $C(A) \sim [AH]$. At higher pH, the relationship between the concentration of acidic species (HA) and the total amount of compounds ($[A] \sim [A^-] + [AH]$) varies with pH and pKa (Brønsted acidity). An apparent octanol partition coefficient can be defined for the whole compound: $P_{APP}(A) = [\sum A]_O/[\sum A]_W$. It may be assumed in a first approach that ionic species remain predominantly in water, and partitioning mainly occurs for the neutral species of the compound. Based on this assumption, the apparent partition coefficient becomes $P_{APP} = ([HA]_{O+0})/([HA]_W + [A^-]_W)$, leading to the following equation:

$$P_{APP}(A) = \frac{P_{OW}(HA)}{1 + 10^{(pH-pK_a)}} \quad \text{Eq. S1}$$

A similar analysis can be performed with dicarboxylic acids leading to an analogue equation:

$$P_{APP}(A) = \frac{P_{OW}(H_2A)}{1 + 10^{(pH-pK_{a1})} \times [1 + 10^{(pH-pK_{a2})}]} \quad \text{Eq. S2}$$

In the present work, P_{OW} and P_{APP} are supposed equal for non ionizable compounds (*e.g.* benzene). On the other hand, the use of P_{APP} is preferred for ionizable compounds (*e.g.* Benzoic acid). However, the previous equations may become wrong for low P_{APP} values ($\log P_{APP} \ll 3$), for example when other mechanisms, such as partitioning of ion pairs, becomes significant. For that reason, we measured experimentally $\log P_{APP}$ values of organic compounds in Tégulines pore water.

Experimental measurement of $\log P_{APP}$:

Experiments for the determination of partition coefficient were performed in an octanol/water system. The octanol was presaturated with water by equilibrating them for 48 hours, corresponding to hydration ratio of 5.64% by mass. The aqueous phase was prepared according to the composition of Tégulines pore water. Experiments were performed at room temperature. Organic compounds were solubilized in one of the two solvent, i.e. either octanol for lipophilic compounds or water for hydrophilic compounds. The Tégulines pore water was added to a vessel containing a magnetic stirrer. Then the octanol (water saturated) was slowly filled upon the aqueous phase. Stirring speed was kept moderate in order to prevent the formation of colloids. The two phases were mixed for 48h before the measurement. After separation, the concentration of organic compounds in each phase was analysed by UV-Vis spectroscopy (Cary 500, Agilent) for o-phthalate, toluene or naphthalene; and by liquid scintillation counting (Wizard Tri-Carb device and ultima-gold® scintillation liquid form Perkin Elmer) for ^{14}C -radiolabeled compounds, oxalate and benzene. Data for lipophilic compounds are in good agreement with references values (**Fig. S1**), thus validating the experimental procedures.

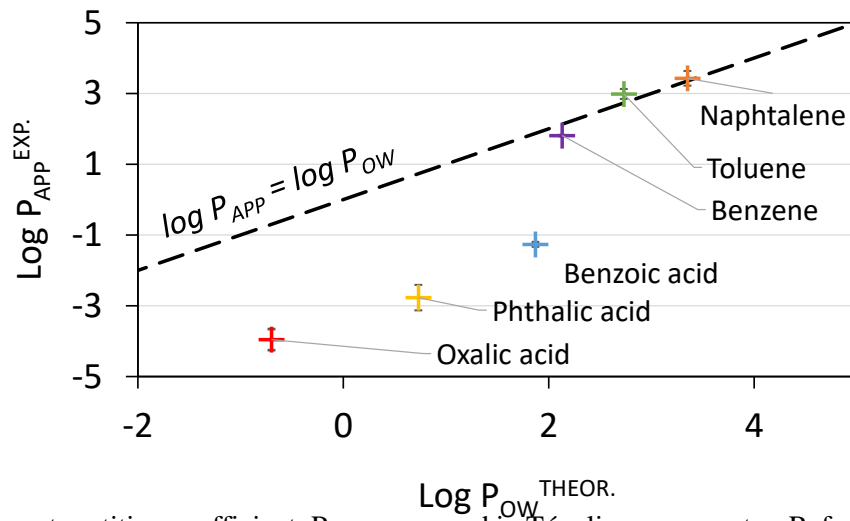


Fig. S1. Apparent partition coefficient, P_{APP} , measured in Tégulines pore water. Reference partition values, P_{OW} , are theoretical and defined for acidic form of carboxylic acids (HA).

Sorption isotherms:

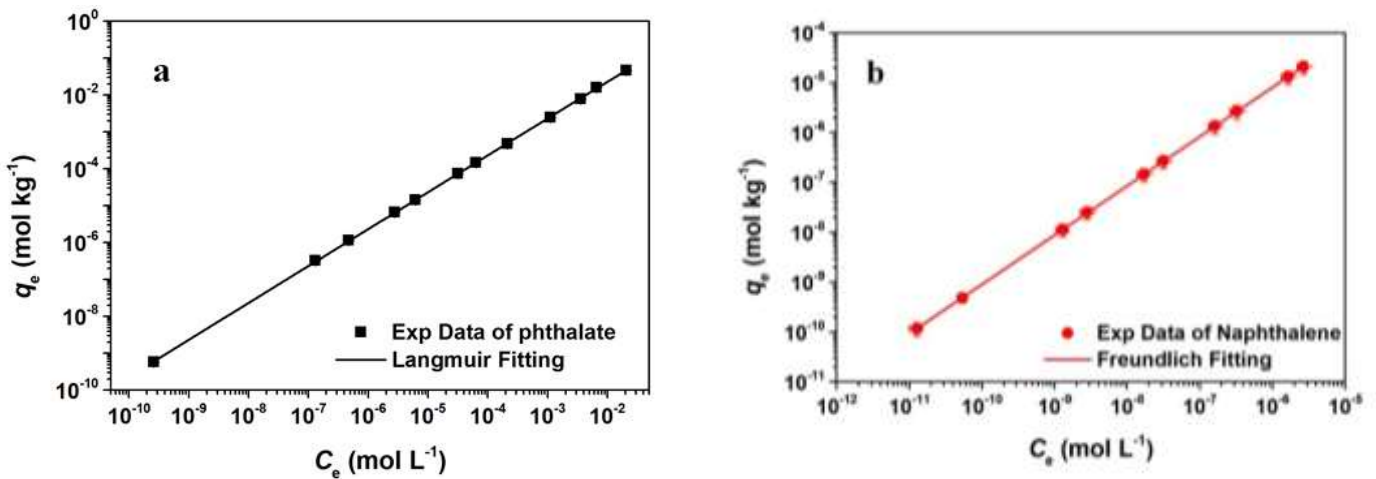


Fig. S2. Sorption isotherm of organic compounds on Tégulines clay rock.
 (a, top) Modelling of o-phthalate sorption isotherm with Langmuir model.
 (b, bottom) Modelling of naphthalene sorption isotherm with Freundlich model.

Through-diffusion experiments

Through-diffusion experiments were performed in diffusion cells in polyether ether ketone (PEEK). The cell geometry and corresponding picture are provided in Fig. S4. Rock samples were pasted with epoxy resin (Sikadur®) between two stainless steel filter plates in contact with upstream/downstream solutions. Prior to diffusion with organic tracers, semi-heavy water (HDO) was injected in upstream compartment and HDO concentration was monitored in both compartments. Hence, HDO was used as a conservative reference, i.e. non sorbing tracer with access to the whole porosity with results given in the following section.

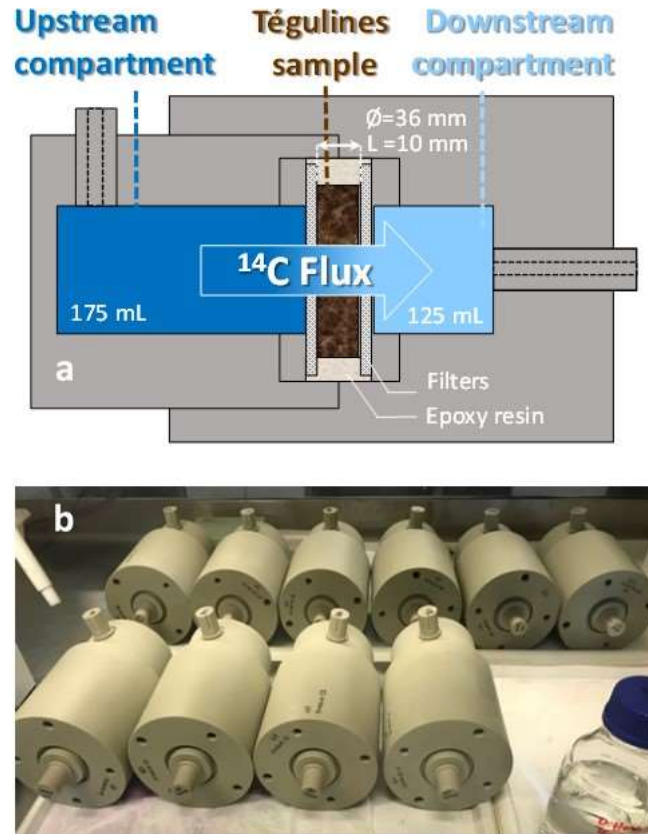


Fig. S3. a) Scheme of the experimental setup for through diffusion experiments
b) Picture of the diffusion cells in anoxic glovebox during hydration step.

Diffusion results with HDO tracer:

The diffusion of water in Tégulines clay rock was investigated for each diffusion cell, by use of deuterium-labelled water (HDO). Accumulated HDO was detected in downstream very soon, and increases fast with time, as seen in Fig. S4. The downstream concentration was normalized by the initial upstream concentration. Different HDO concentrations were measured in different cells at the same time due to the discrepancies of different clay rock sample disks, such as length and surface of the sample disk. On the purpose to eliminate this effect, Eq. 8 and 9 were used to obtain the normalized flux. The normalized downstream flux (symbols in Fig. S4, c) raises rapidly through the transitory state in one day and then achieves a plateau, which represents the effective diffusion coefficient (D_e) of HDO. D_e and α values can be obtained by the best fitting of the normalized flux using Fick's second law. The best fit values used to simulate the depletion concentration of upstream compartment provide an acceptable agreement (Fig. S4).

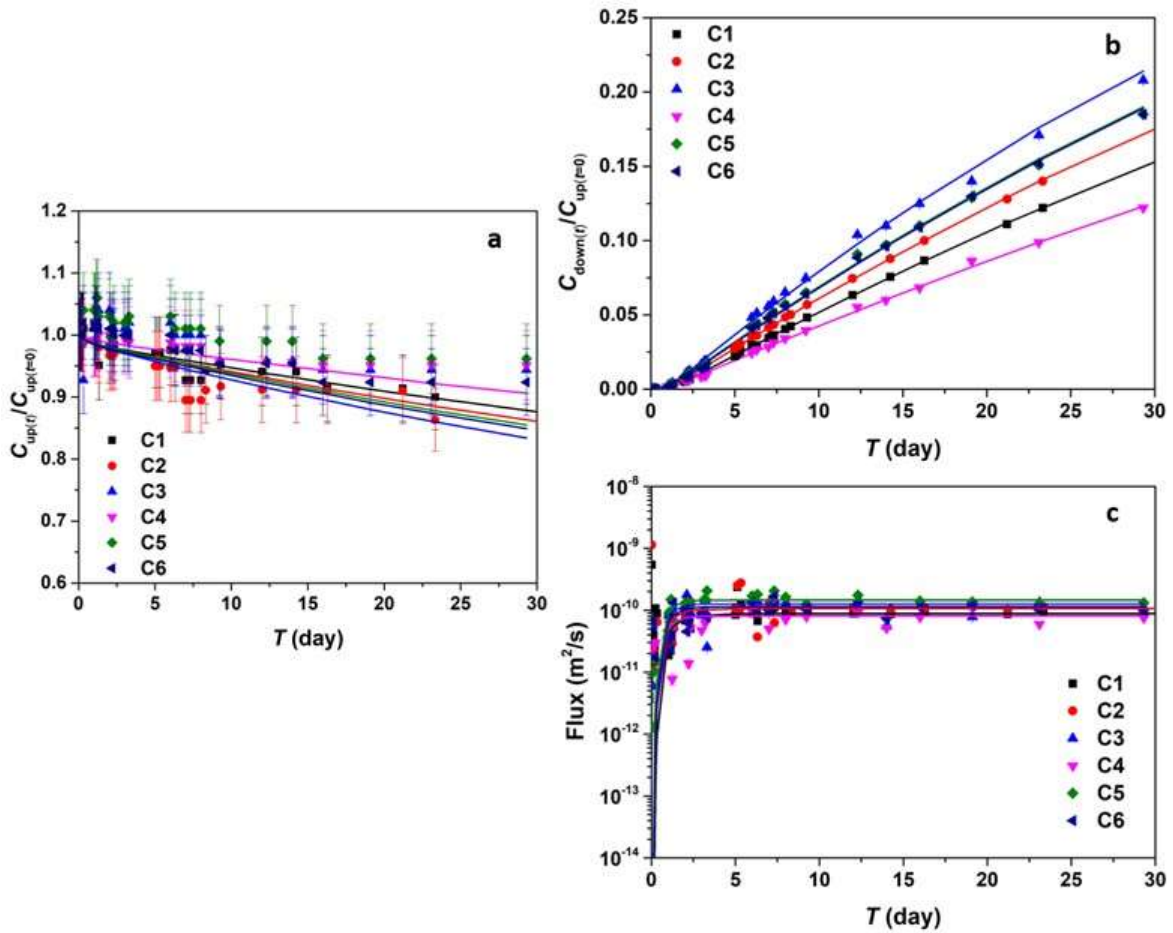


Fig. S4. HDO Diffusion results for Tégulines diffusion cells #1 to #6. (a) Upstream and (b) Downstream concentration are normalized by initial upstream concentration, $C_{up(t0)}$. (c) Downstream fluxes, normalized by $\Delta L/C_{up(t0)}$ and used for adjustment of modelling (solid lines).

Through-diffusion experiments with organic compounds:

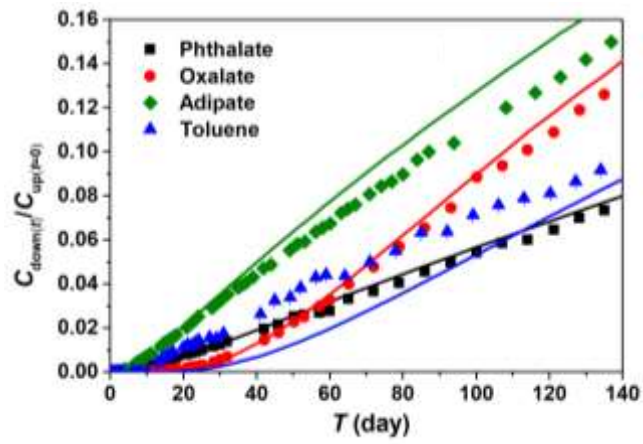
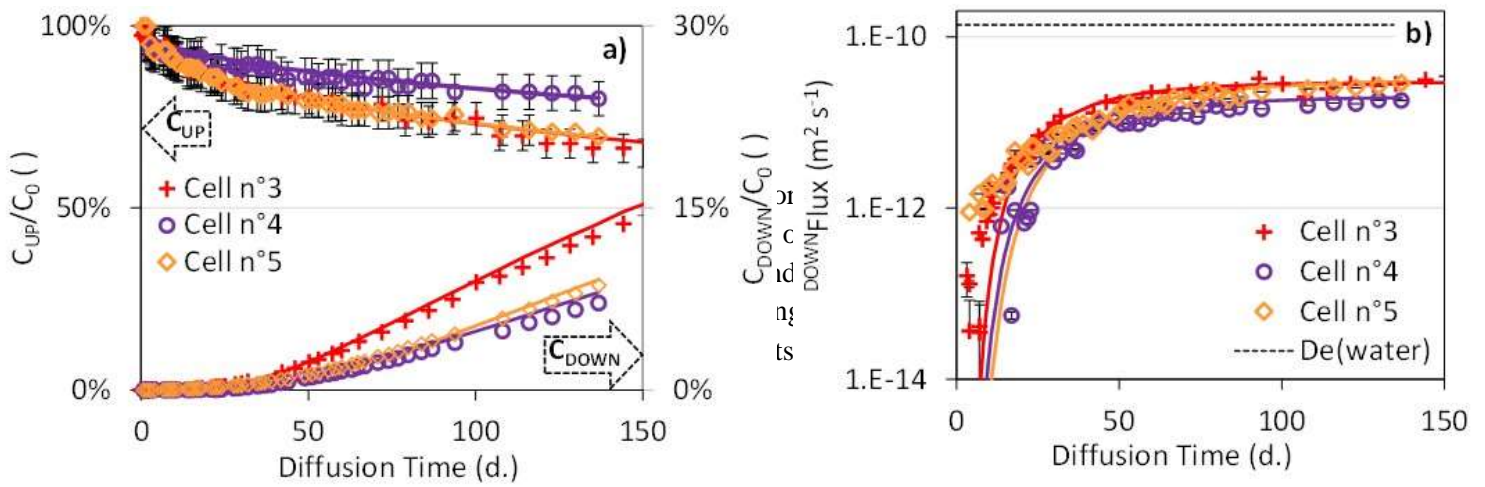


Fig. S5. Diffusion of organic compounds in Tégulines clay rock. Cumulative concentration in downstream compartment as a function of diffusion time.



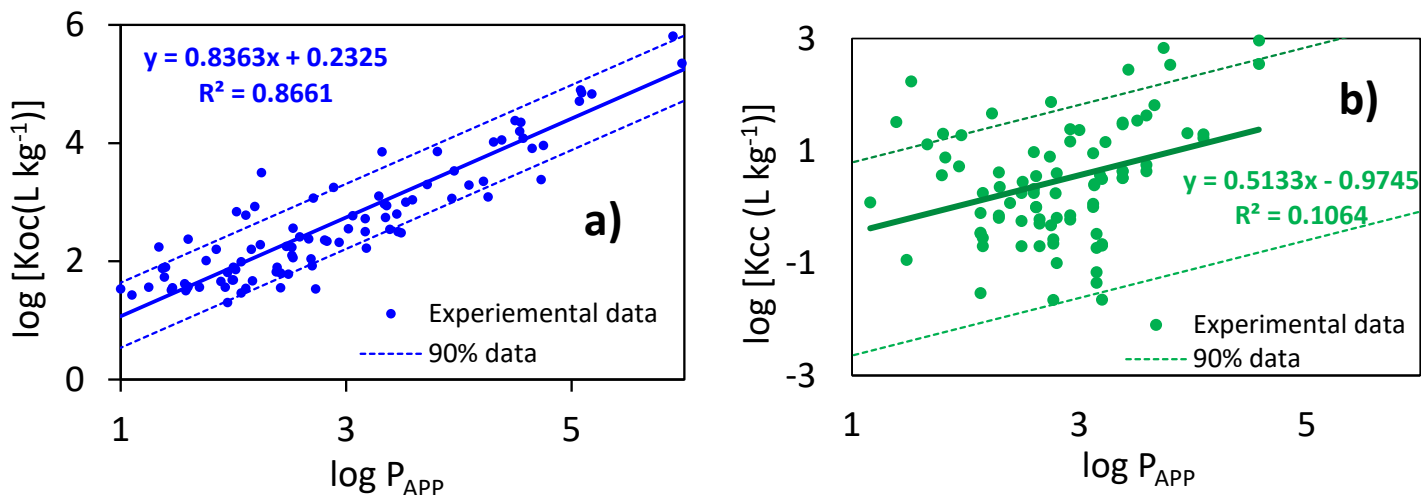


Fig. S7. Sorbent contribution to the solid-liquid distribution coefficient for lipophilic compounds.

a) Values reported per organic content of the media: $K_{oc}(\text{L kg}(\text{NOM})^{-1}) = R_d / f_{oc}$.

Data from references Karickhoff et al., 1981; Borisover et al., 1997; Serrano et al., 2006.

b) Values reported per clay content of the media: $K_{cc}(\text{L kg}(\text{clay minerals})^{-1}) = R_d / f_{CM}$.

Data from references Larsen et al., 1992, Pennell et al., 1992; Li and Gupta, 1994; Gawlik et al., 1998;

Rowe et al., 2005; on pure clay minerals or aquifers materials with very low OC ($\ll 1\%$).

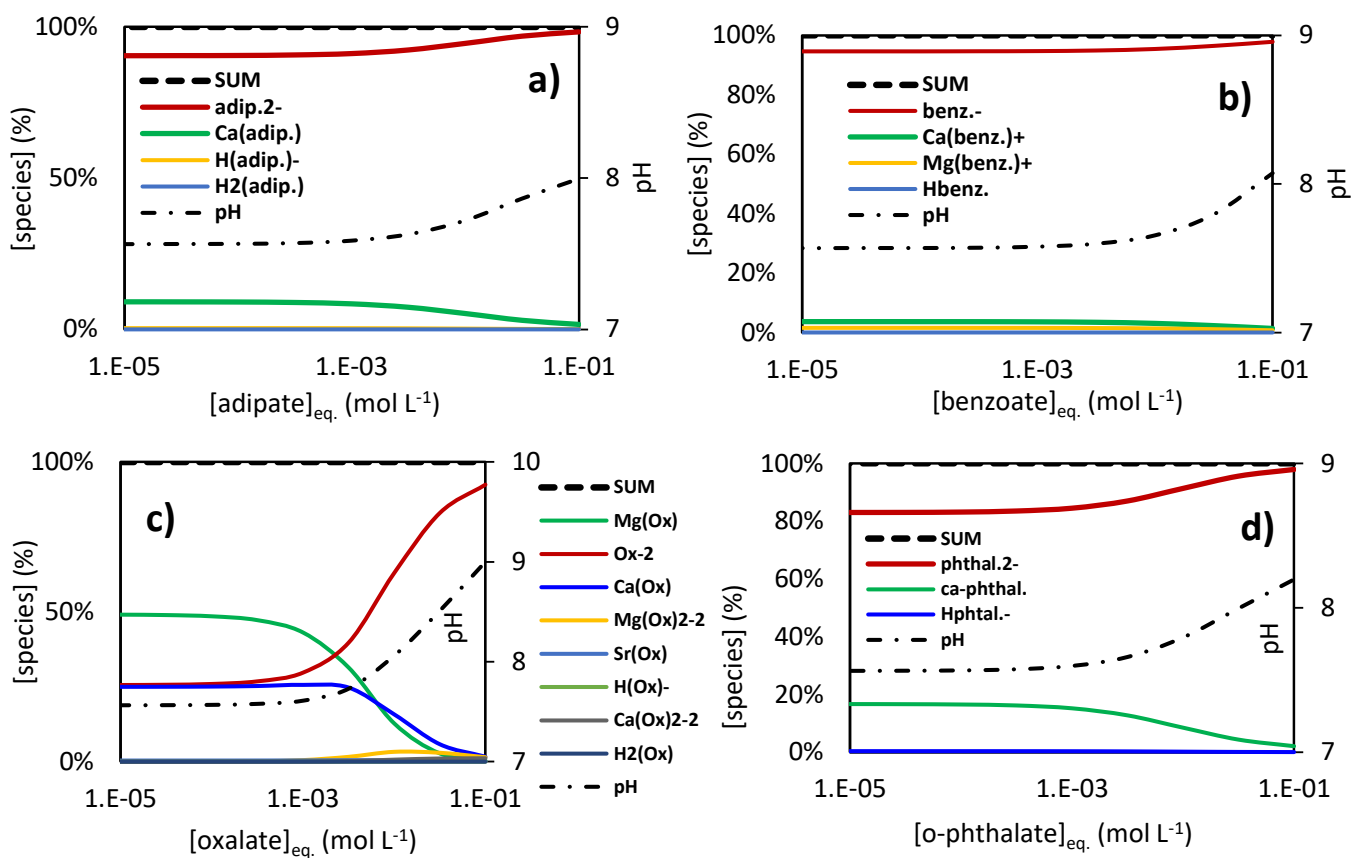


Fig. S8. Speciation calculations in Tégulines pore water. $T = 25\text{ }^\circ\text{C}$, $\text{pH} \sim 7$, equilibrium with calcite ($\text{CaCO}_{3(s)}$) imposed. Speciation data are reported as a function of equilibrium concentrations for a) Adipic acid, b) Benzoic acid, c) Oxalic acid, d) Ortho-phthalic acid.

Bibliographic references:

- Borisover, M.D., Graber, E.R., 1997. Specific interactions of organic compounds with soil organic carbon. ACS Div. Environ. Chem. Prepr. 37, 172–174.
- Gawlik, B.M., Feicht, E.A., Karcher, W., Kettrup, A., Muntau, H., 1998. Application of the European reference soil set (EUROSOILS) to a HPLC-screening method for the estimation of soil adsorption coefficients of organic compounds. Chemosphere, 36, 14, 2903-2919.
- Heilman, M.D., Carter, D.L., Gonzalez, C.L. 1965. The ethylene glycol monoethyl ether (EGME) technique for determining soil-surface area. Soil Science 100, 409–413.
- Karickhoff, S.W., 1981. Semi-empirical estimation of sorption of hydrophobic pollutants on natural sediments and soils. Chemosphere, 10 (8), 833–846.
- Larsen, T., Kjeldsen, P., Christensen, T.H., 1992. Sorption of hydrophobic hydrocarbons on three aquifer materials in a flow through system. Chemosphere, 24, 4, 439-451.
- Li, L., Gupta, G. 1994. Adsorption/desorption of hydrocarbons on clay minerals. Chemosphere, 28, 3, 627-638.
- Pennell, K.D., Dean Rhue, R., Suresh, P., Rao, C., Johnston, C.T., 1992. Vapor-phase sorption of p-xylene and water on soils and clay minerals. Environ. Sci. Tech.26, 756-763.
- Rowe, R.K., Mukunoki, T., Sangam, H.P., BTEX Diffusion and Sorption for a Geosynthetic Clay Liner at Two Temperatures. J. Geotech. Geoenviron. Eng., 131, 1211-1221.
- Serrano, A., Gallego, M. 2006. Sorption study of 25 volatile organic compounds in several Mediterranean soils using headspace–gas chromatography–mass spectrometry. Journal of Chromatography A, 118, 2, 23, 261-270.